

Supplementary Material

Investigation of selective microwave heating phenomena in the reactions of 2-substituted pyridines

Péter Bana,^A István Greiner^{B,C}

^A Department of Organic Chemistry and Technology,
Budapest University of Technology and Economics, H-1521 Budapest, Hungary.

^B Gedeon Richter Plc., H-1475 Budapest, PO Box 27, Hungary.

^C Corresponding author. Email: i.greiner@richter.hu

Table of contents

Equipment for oil bath and microwave (MW) heating experiments	S2
Technical details of recording the temperature signal.....	S4
Calibration of the temperature sensors.....	S4
Measurement of MW power levels	S4
Preparation of 2-(benzyloxy)pyridine (3).....	S5
Spectral data of 2-(benzyloxy)pyridine (3)	S6
Harmonized temperature profiles in the rearrangement of 2-(benzyloxy)pyridine.....	S7
IR controlled MW heating of the rearrangement of 2-(benzyloxy)pyridine	S9
IR controlled MW heating of incomplete reaction mixtures of the rearrangement of 2-(benzyloxy)pyridine....	S10
Analysis of the reaction mixtures of the rearrangement of 2-(benzyloxy)pyridine.....	S11
Spectral data of the product (4) of the rearrangement of 2-(benzyloxy)pyridine.....	S12
Preparation of 2-(benzyloxy)-1-methylpyridinium trifluoromethanesulfonate (S1).....	S14
Preparation of 2-(benzyloxy)-1-methylpyridinium tetrakis[3,5-bis(trifluoromethyl)phenyl]borate (1).....	S14
Spectral data of the prepared 2-(benzyloxy)-1-methylpyridinium salts	S16
MW heating characteristics of the quartz vessels	S20
Harmonized temperature profiles in the benzylation of <i>p</i> -xylene	S21
Analysis of the reaction mixtures of the benzylation of <i>p</i> -xylene.....	S23
Observation of 1,3-bis(trifluoromethyl)benzene (9) in the vapors.....	S26
Spectral data of the product (6) of the benzylation of <i>p</i> -xylene	S26
References.....	S28

Equipment for oil bath and microwave (MW) heating experiments

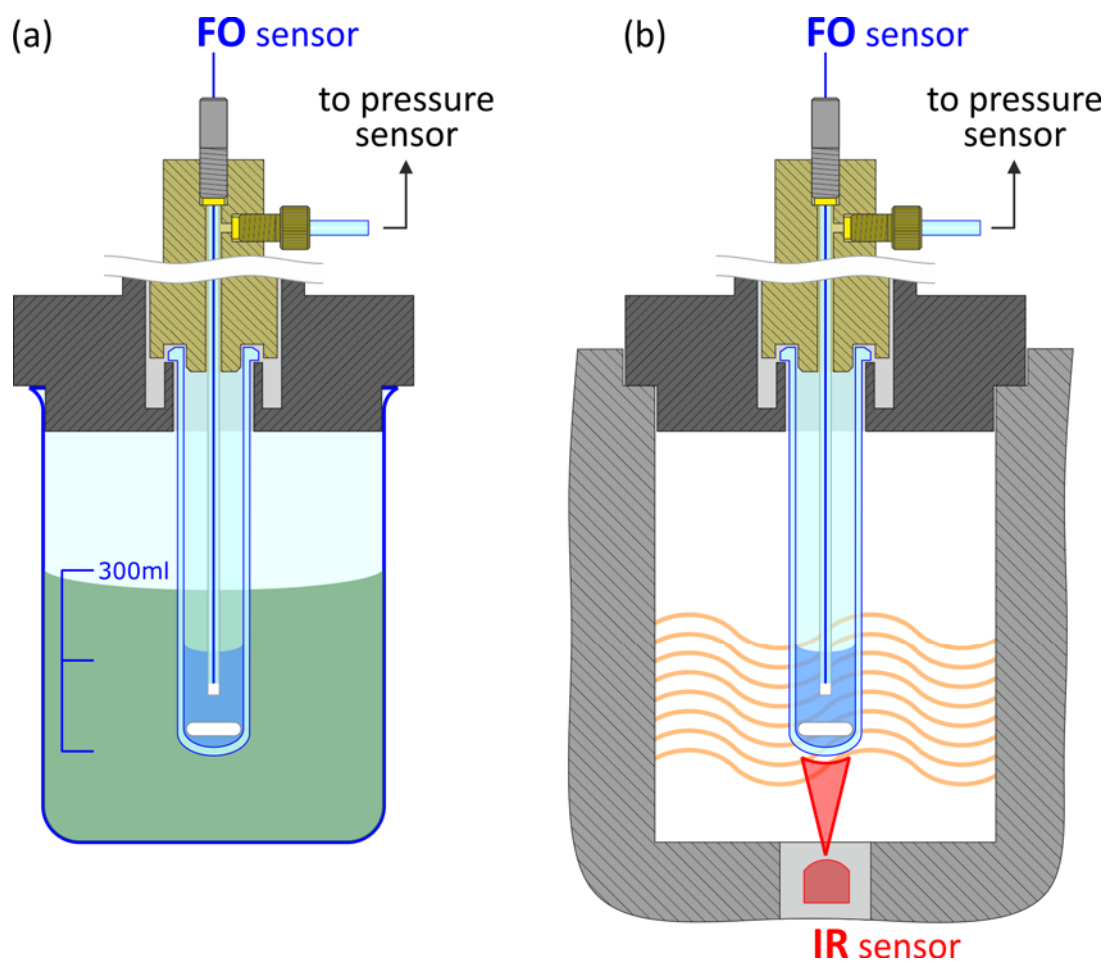


Fig. S1. Experimental set-up (simplified schematic) consisting of oil bath (a) and MW (b) heating of geometrically identical reaction vessels, showing the position of the fiber optic (FO) thermometer and infrared (IR) pyrometer.

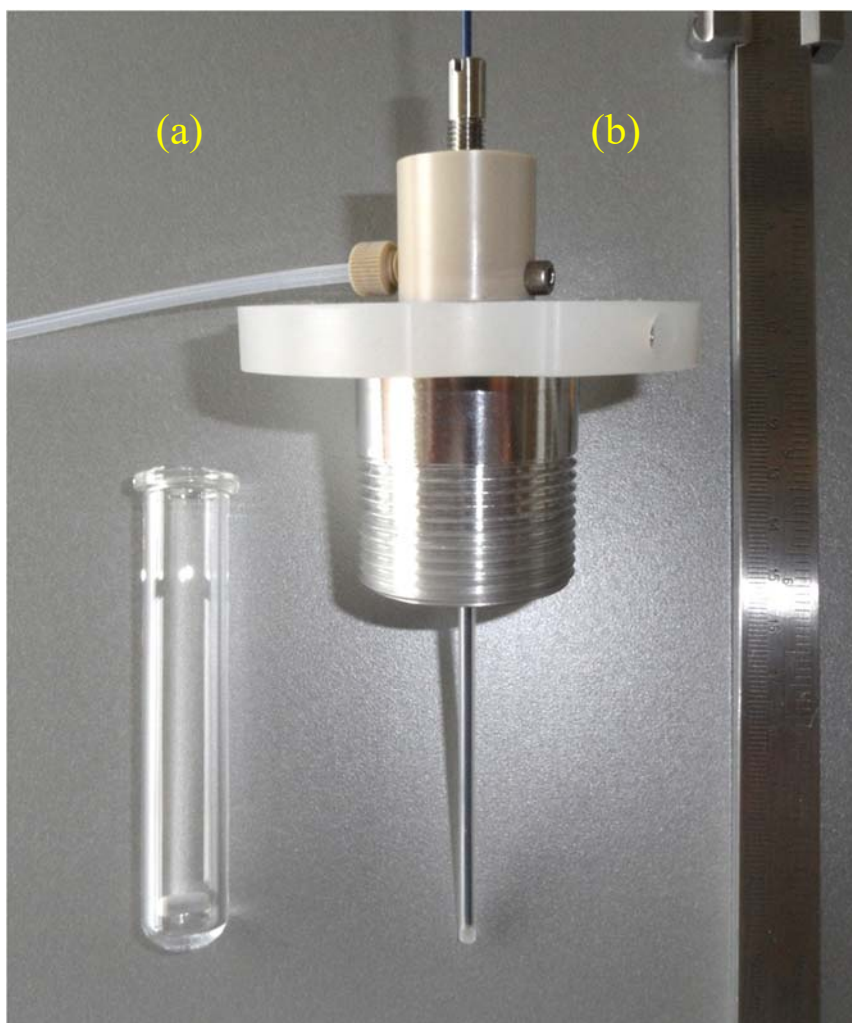


Fig. S2. Photograph of the 10 mL volume cylindrical Pyrex[®] MW reaction vessel with stir bar (a) and the locking cover assembly with the FO sensor inside the glass thermowell (b) as used throughout this study.

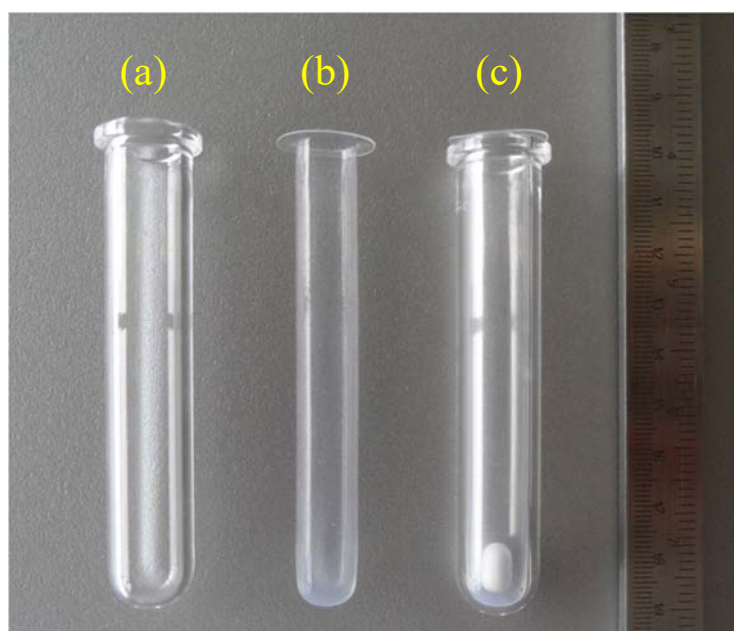


Fig. S3. Photograph of the 10 mL volume cylindrical quartz MW reaction vessel (a), the Teflon[®] PFA liner (b) and the assembled vessel with the liner and stir bar (c) as used in the benzylation of *p*-xylene.

Technical details of recording the temperature signal

In oil bath heated set-up, the fiber optic (FO) sensor's signal was recorded through the CEM Discover[®] MW instrument, in order to exclude any errors from the different read-out instrumentation.

In the FO controlled MW experiments (besides the FO temperature) the signal of the infrared (IR) temperature sensor in the same MW reactor was also monitored simultaneously, using the data that can be extracted from the IP packets sent on the LAN connection between the instrument and the controlling PC.

In the IR controlled MW experiments (the MW reactor's own FO sensor is inactive by design) a secondary CEM Discover[®] equipment of the same type was used for simultaneous FO temperature measurement. The IR temperature and applied MW power is recorded through the primary MW reactor, the secondary instrument acts as signal transducer to monitor FO temperature and pressure of the reaction mixture.

Calibration of the temperature sensors

The factory calibration of FO sensor was checked by measuring the boiling temperature of a stirred samples of distilled water (100 °C), 1-butanol (117 °C), *N,N*-dimethylformamide (153 °C) and ethylene glycol (196 °C). The calibration was found to be precise (within 2 °C) and stable, no modification was needed.

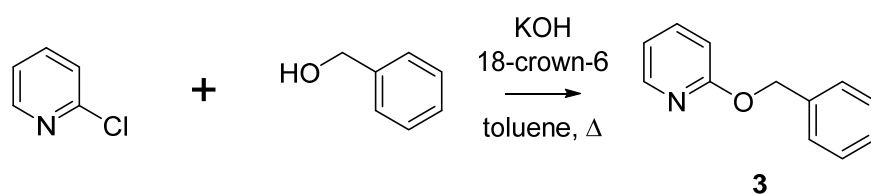
The built-in IR sensor was regularly calibrated. A stirred sample of *N,N*-dimethylformamide (25 mL) was boiled using continuous MW irradiation in a 50 mL round-bottom flask under reflux condenser, until stable reflux and constant temperature reading (for at least 5 minutes) was reached. The calibration was adjusted so the boiling temperature is measured as 153 °C. The accuracy and linearity of the calibration was checked by measuring the boiling temperature (continuous MW irradiation while stirring, until reaching stable reflux and constant reading for at least 5 minutes) of samples of distilled water (100 °C), 1-butanol (117 °C), *N,N*-dimethylformamide (153 °C) and ethylene glycol (196 °C) in round-bottom flasks under reflux condenser. The calibration was found to be precise (within 2 °C) and linear in the relevant range.

The same procedure was repeated using 10 mL volume cylindrical quartz reaction vessels fitted with a reflux condenser. Samples (2 mL) of distilled water and 1-butanol gave identical results.

Measurement of MW power levels

The actual power levels in our MW reactors were tested using the protocol provided by the manufacturer. In a 100 mL round bottom flask 100 mL of distilled water is irradiated for 60 seconds at 300 W fixed power setting. The power is calculated based on the temperature change. All of the values were in the acceptable range.

Preparation of 2-(benzyloxy)pyridine (**3**)^[S1]



Scheme S1. Preparation of 2-(benzyloxy)pyridine.

A 500-mL round-bottomed flask equipped with magnetic stir bar and Dean-Stark trap with reflux condenser was charged with benzyl alcohol (11.7 g, 0.108 mol, 1.0 equiv.), 2-chloropyridine (13.5 g, 0.119 mol, 1.1 equiv.), freshly ground potassium hydroxide (20.0 g, 0.356 mol, 3.3 equiv.), 18-crown-6 (1.43 g, 5.40 mmol, 0.05 equiv.) and toluene (210 mL). The reaction mixture was heated to reflux with azeotropic removal of water for 1 h.

Water (100 mL) was added to the cooled reaction mixture and the organic phase was separated, washed with water (2x100 mL) and concentrated under reduced pressure.

The crude product was purified by vacuum distillation (bp. 97–101 °C, 1.1 mmHg) providing 17.3 g (86%) of 2-(benzyloxy)pyridine (**3**) as a colorless liquid.

Spectral data (Fig. S4) were found to be identical to the literature.^[S1]

¹H NMR: δ_{H} (400 MHz, CDCl_3) 8.18 (1 H, dd, J 5.0, 1.3), 7.58 (1 H, ddd, J 8.8, 7.2, 1.9), 7.49 – 7.44 (2 H, m), 7.41 – 7.34 (2 H, m), 7.34 – 7.28 (1 H, m), 6.88 (1 H, ddd, J 6.9, 5.1, 0.7), 6.81 (1 H, d, J 8.4), 5.38 ppm (2 H, s);

¹³C NMR: δ_{C} (101 MHz, CDCl_3) 163.59, 146.80, 138.58, 137.32, 128.42, 127.91, 127.77, 116.87, 111.30, 67.49 ppm.

Spectral data of 2-(benzyloxy)pyridine (**3**)

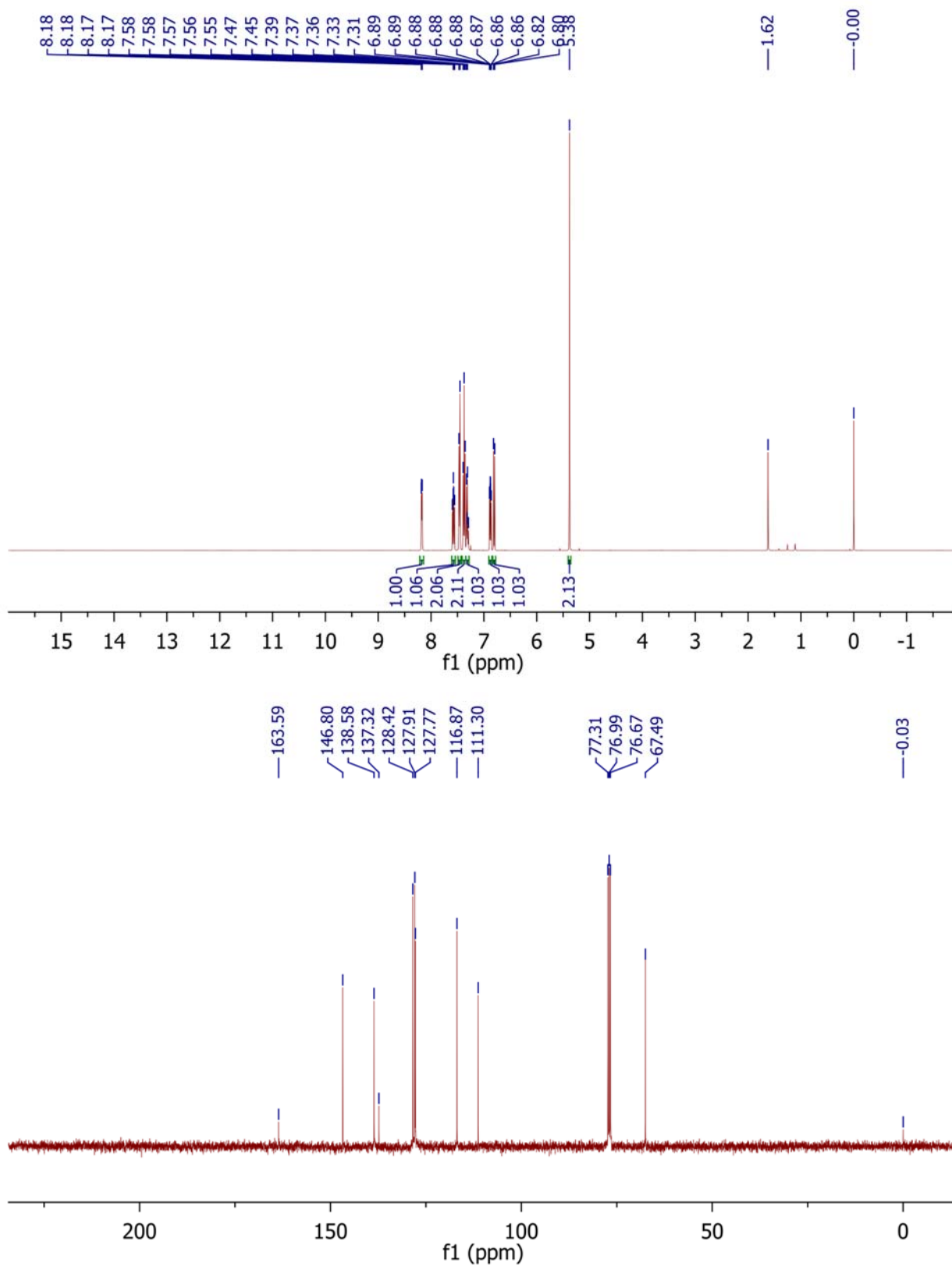
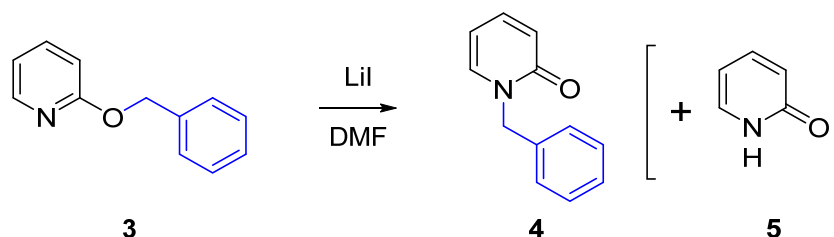


Fig. S4. $^1\text{H-NMR}$ and $^{13}\text{C-NMR}$ spectra (400 MHz, CDCl_3) of 2-(benzyloxy)pyridine.

Harmonized temperature profiles in the rearrangement of 2-(benzyloxy)pyridine



Scheme S2. Rearrangement of 2-(benzyloxy)pyridine.

Conventional heating for 50 min total time using pre-heated oil bath (220 °C) was conducted, the obtained inner temperature profile (Fig. S5) was recreated in the MW reactor after extensive experimentation. The set temperature (200 °C) was identical to the steady-state temperature reached in the oil bath experiment, the power settings leading to the best fit are described in Table S1.

Table S1. Harmonized temperature profiles in the rearrangement of 2-(benzyloxy)pyridine.

Entry	Heating (control) mode	power setting	mean power ^A	heat-up time ^B	mean FO temp. ^A	mean IR temp. ^A
1	MW heating (IR control, 200 °C)	25 W	11 W	74 s	229.5 °C	195.6 °C
2	Conventional heating (FO monitoring)	–	–	92 s	197.6 °C	–
3	MW heating (FO control)	25 W	11 W ^C	93 s ^C	197.3 °C ^C	192.3 °C ^C
4	MW heating simultaneous cooling (FO control)	100 W	67 W ^C	54 s ^C	198.5 °C ^C	165.7 °C ^C
5	MW heating (IR control, 180 °C)	25 W	6 W	–	212.5 °C	176.2 °C
6	MW heating (IR control, 160 °C)	25 W	3 W	–	192.0 °C	157.4 °C

^A Mean value is calculated for the total heating time (0 – 3000 s).

^B Heat-up time is the time interval until reaching 180 °C (measured by FO sensor).

^C Average of parallel experiments (n=3).

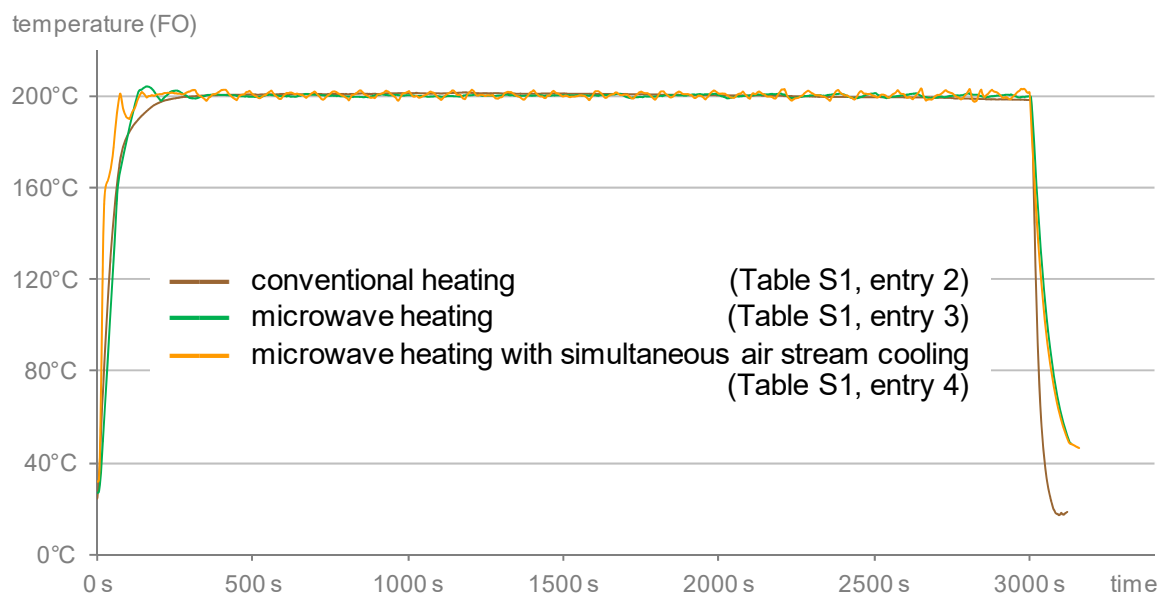


Fig. S5. Comparison of the internal temperature profiles of conventionally and MW heated mixtures of 2-(benzyloxy)pyridine in DMF. The temperatures were measured during the course of the reaction by the FO sensor. Temperature profiles of the parallel experiments (not shown for clarity reasons) are in good accordance with the displayed profiles.

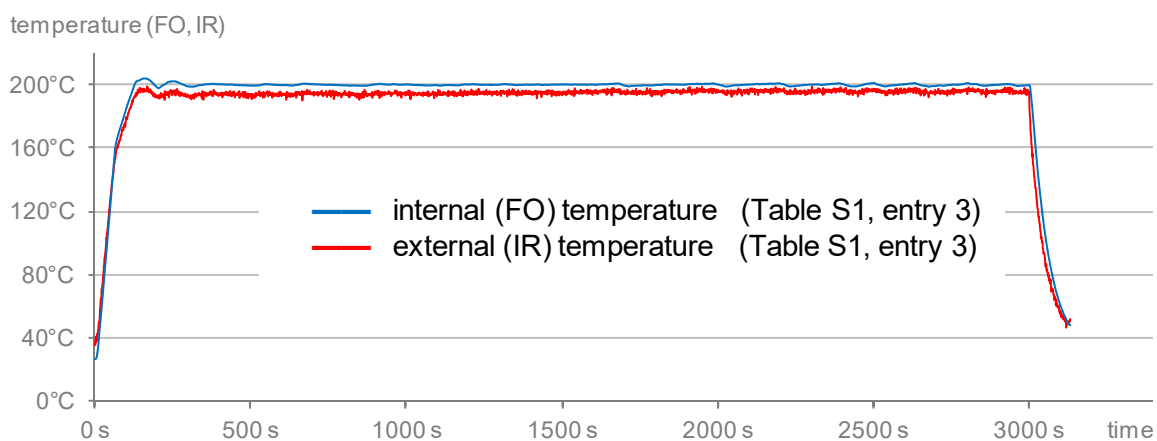


Fig. S6. Comparison of the internal (FO) and external (IR) temperature profiles of MW heated (FO control) mixtures of 2-(benzyloxy)pyridine in DMF.

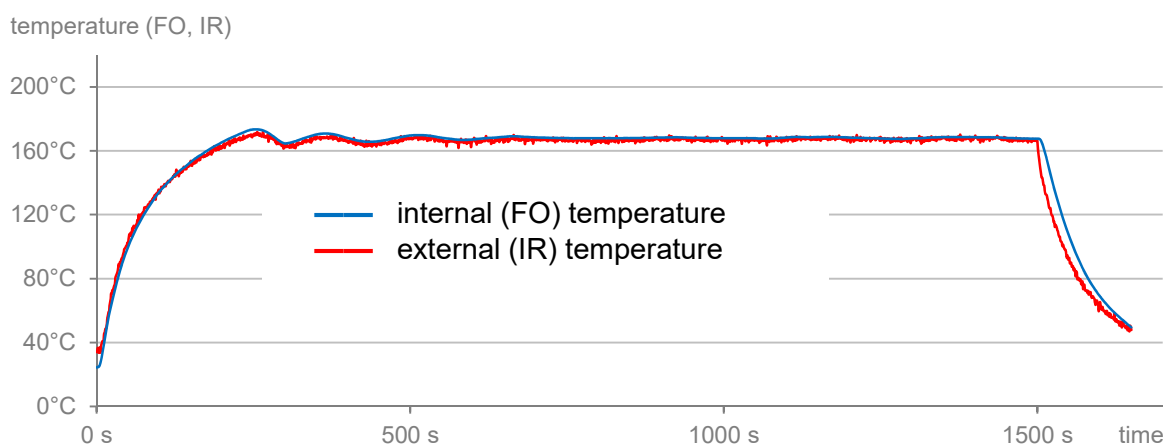


Fig. S7. Comparison of the internal (FO) and external (IR) temperature profiles of MW heated (FO control) mixtures of 2-chloropyridine and piperidine, which was conducted in our previous study.^[S2]

IR controlled MW heating of the rearrangement of 2-(benzyloxy)pyridine

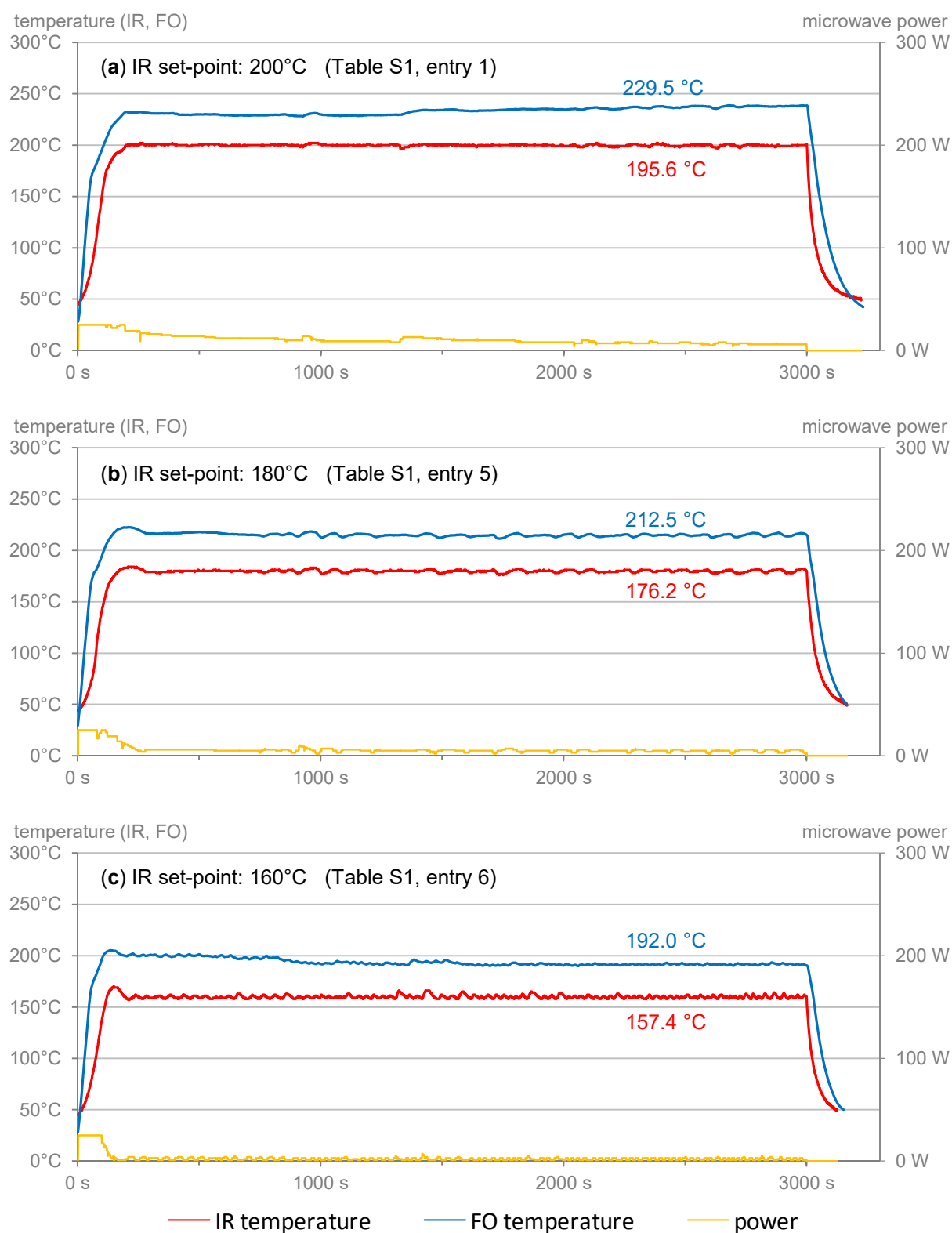
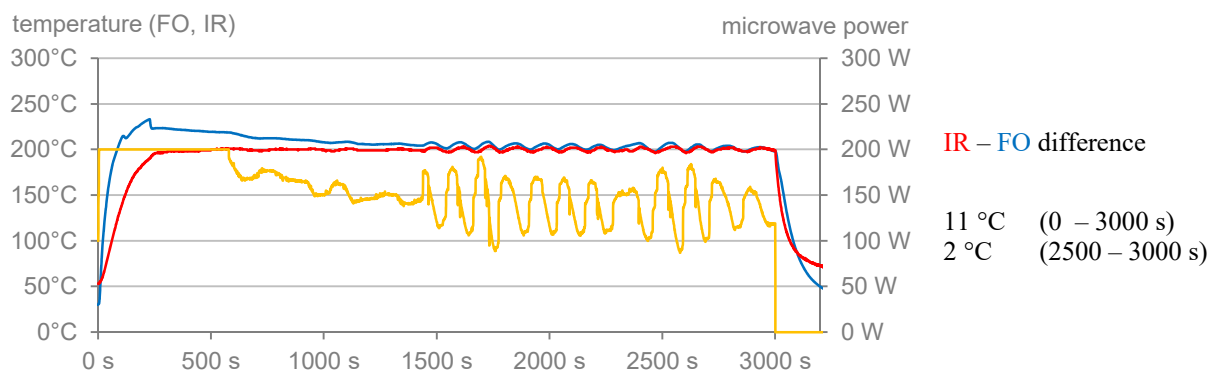


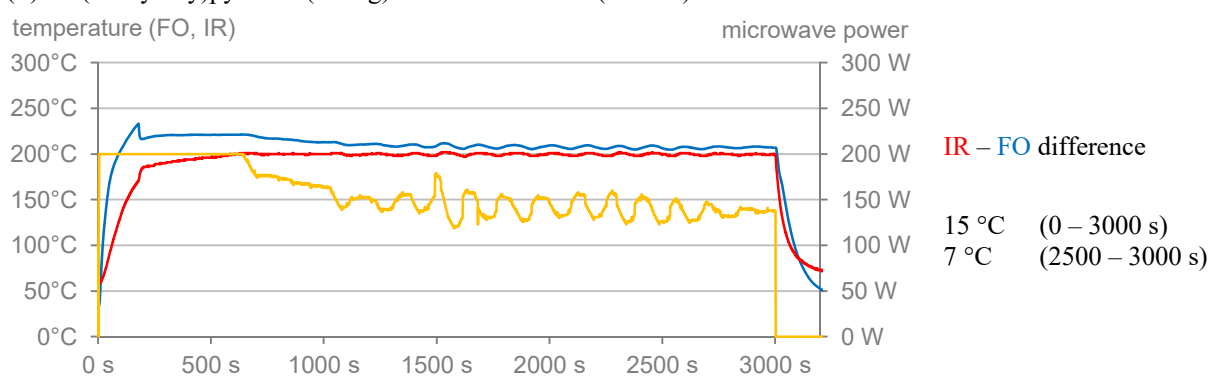
Fig. S8. Temperature measured by the IR and FO sensors simultaneously during the IR controlled MW heated rearrangement of 2-(benzyloxy)pyridine in DMF. Mean reaction temperatures (0 – 3000 s) are indicated for both sensors ((a): 195.6 °C and 229.5 °C respectively; (b): 176.2 °C and 212.5 °C respectively; (c): 157.4 °C and 192.0 °C respectively).

IR controlled MW heating of incomplete reaction mixtures of the rearrangement of 2-(benzyloxy)pyridine

(a) DMF (2.0 mL)



(b) 2-(benzyloxy)pyridine (96 mg) dissolved in DMF (2.0 mL)



(c) Lithium iodide (104 mg) dissolved in DMF (2.0 mL)

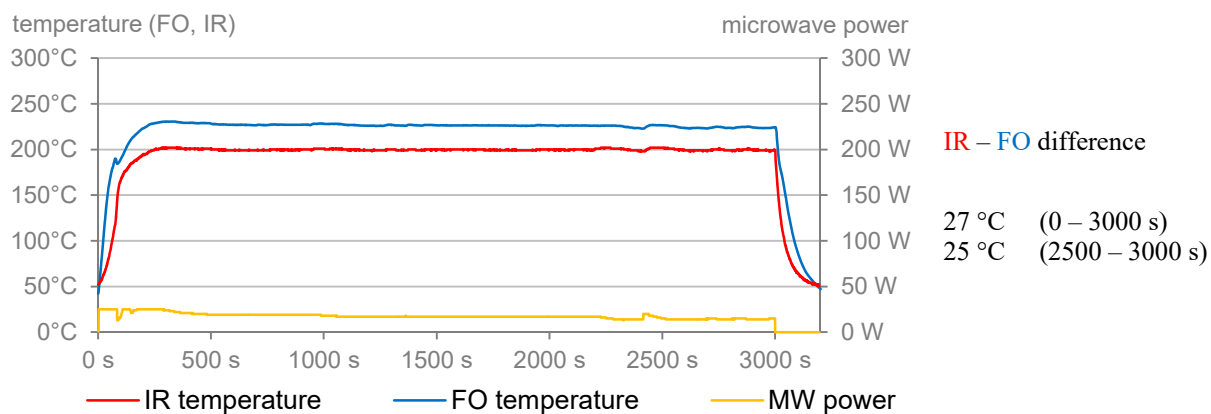


Fig. S9. Difference between IR and FO temperatures in IR controlled MW heating of incomplete reaction mixtures of the rearrangement of 2-(benzyloxy)pyridine (conditions: 200 °C set temperature, 50 min total time, 25 or 200 W MW power).

Analysis of the reaction mixtures of the rearrangement of 2-(benzyloxy)pyridine

Conversion, based on the $^1\text{H-NMR}$ spectra of the crude reaction mixtures (Fig. S10), was calculated using the integrated intensity (I) of peaks at 5.21 ppm (P ; N -benzyl-2-pyridone product, $N\text{-CH}_2\text{-Ph}$) and 6.44 ppm (BP ; 2-pyridone by-product, $C3\text{-H}$) compared to 5.37 ppm (SM ; 2-(benzyloxy)pyridine starting material, $O\text{-CH}_2\text{-Ph}$):

$$\text{conversion(\%)} = \frac{I(P) + 2 \cdot I(BP)}{I(P) + 2 \cdot I(BP) + I(SM)}$$

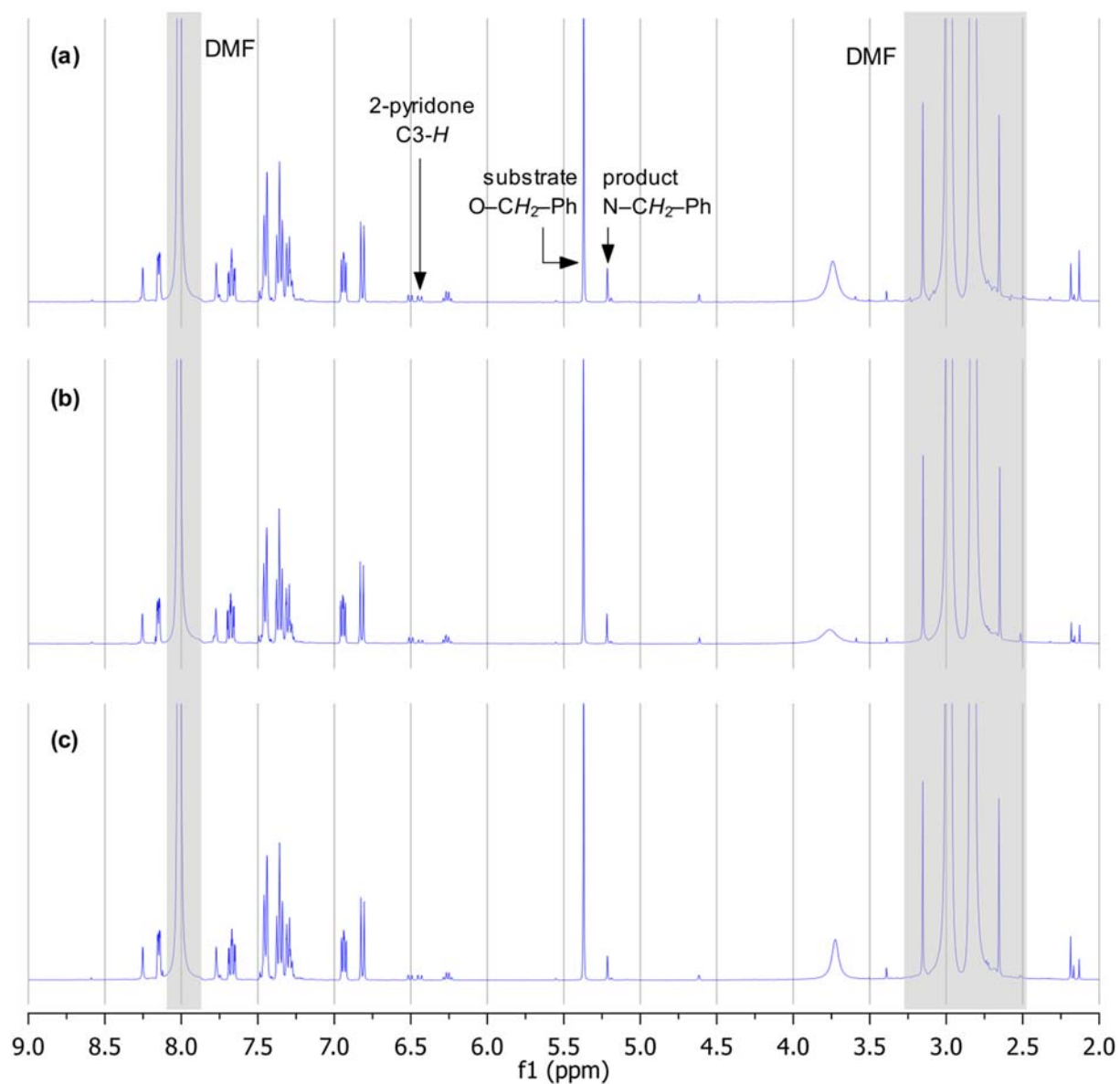


Fig. S10. $^1\text{H-NMR}$ spectra (9.0 – 2.0 ppm) of crude reaction mixtures of the conventionally heated (a), FO controlled MW heated (b) and FO controlled MW heated with simultaneous cooling (c) experiments of rearrangement of 2-(benzyloxy)pyridine (conditions: 200 °C, 50 min total time). The diagnostic signals are marked.

Spectral data of the product (4) of the rearrangement of 2-(benzyloxy)pyridine

The spectra (Figure S11) of a purified sample of the reaction product (4) were identical to that of literature reports.^[S3]

¹H NMR: δ_{H} (400 MHz, CDCl₃) 7.38 – 7.22 (7 H, m), 6.61 (1 H, d, *J* 9.1), 6.14 (1 H, td, *J* 6.7, 1.2), 5.15 ppm (2 H, s);

¹³C NMR: δ_{C} (101 MHz, CDCl₃) 162.65, 139.36, 137.17, 136.32, 128.84, 128.08, 127.96, 121.21, 106.18, 51.83 ppm.

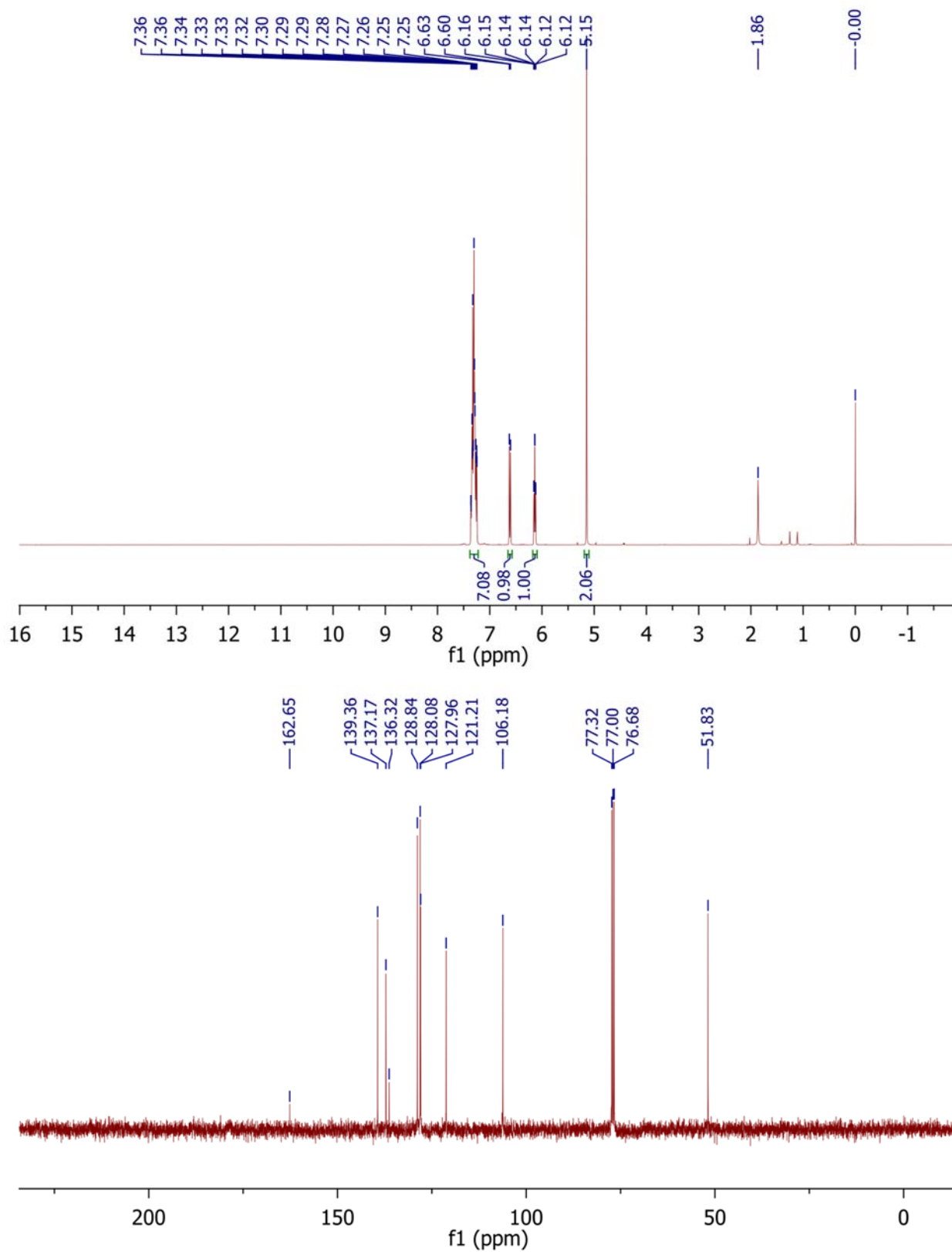
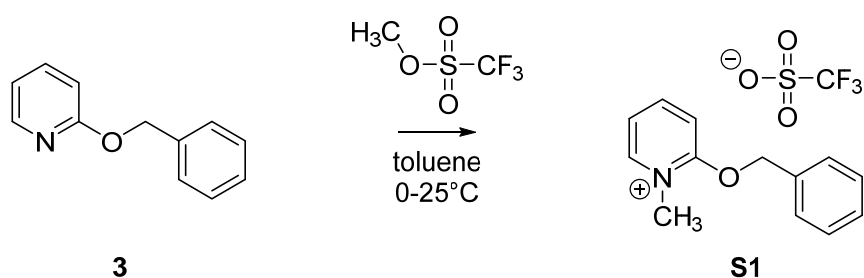


Fig. S11. $^1\text{H-NMR}$ and $^{13}\text{C-NMR}$ spectra (400 MHz, CDCl_3) of a purified sample of the product (4) of the rearrangement of 2-(benzyloxy)pyridine.

Preparation of 2-(benzyloxy)-1-methylpyridinium trifluoromethanesulfonate (**S1**)^[S1]



Scheme S3. Preparation of 2-(benzyloxy)-1-methylpyridinium trifluoromethanesulfonate.

A dry, three-necked, 50 mL, round-bottomed flask equipped with nitrogen bubbler inlet, thermometer, rubber septum and magnetic stir bar was charged with 2-(benzyloxy)pyridine (**3**; 2.2 g, 11.9 mmol, 1.0 equiv.) and toluene (12 mL). The resulting solution was cooled to 0 °C in an ice bath. Methyl trifluoromethanesulfonate (1.4 mL, 12.4 mmol, 1.05 equiv.) was added dropwise via syringe over 10 min, while temperature was kept under 5 °C.

The ice bath was removed and the viscous slurry was allowed to warm to ambient temperature. After 1 h, the heterogeneous reaction mixture was diluted with 10 mL of *n*-hexane and the resulting solids were filtered, washed with one additional portion of *n*-hexane (10 mL) and dried under vacuum, providing 4.05 g (98%) of 2-(benzyloxy)-1-methylpyridinium trifluoromethanesulfonate (**S1**) as a white solid.

All analytical data were found to be identical to the literature.^[S1,S4,S5]

¹H NMR: δ_H (400 MHz, DMSO-*d*₆) 8.72 – 8.67 (1 H, m), 8.57 – 8.48 (1 H, m), 7.83 (1 H, d, *J* 8.8),

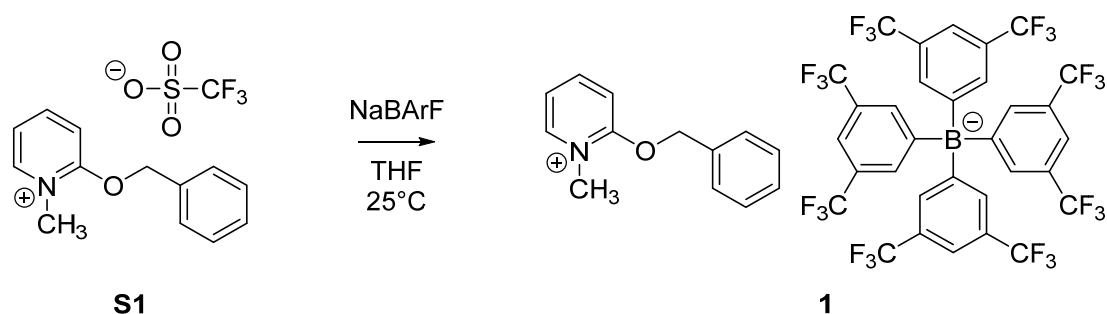
7.62 – 7.54 (3 H, m), 7.52 – 7.40 (3 H, m), 5.63 (2 H, s), 4.01 ppm (3 H, s);

¹³C NMR: δ_C (101 MHz, DMSO-*d*₆) 159.32, 147.67, 143.87, 133.75, 129.04, 128.79, 128.25, 118.56, 111.94,

73.37, 41.51 ppm;

¹⁹F NMR: δ_F (376 MHz, DMSO-*d*₆) -77.79 ppm.

Preparation of 2-(benzyloxy)-1-methylpyridinium tetrakis[3,5-bis(trifluoromethyl)phenyl]borate (**1**)^[S5,S6]



Scheme S4. Preparation of 2-(benzyloxy)-1-methylpyridinium tetrakis[3,5-bis(trifluoromethyl)phenyl]borate.

2-(benzyloxy)-1-methylpyridinium triflate (**S1**; BnOPT, 200 mg, 0.57 mmol) and dry THF (12 mL) was stirred at 40 °C for 15 minutes to obtain a clear solution, which was added to the solution of sodium tetrakis[3,5-bis(trifluoromethyl)phenyl]borate (NaBARF, 500 mg, 0.56 mmol) in dry THF (9 mL). The resulting homogeneous mixture was allowed to stir at room temperature under nitrogen overnight.

The reaction mixture was concentrated under reduced pressure, α,α,α -trifluorotoluene (10 mL) was added, the precipitate was removed by filtration. The solid was washed with α,α,α -trifluorotoluene (2x5 mL). The combined mother liquors were concentrated under reduced pressure to 5 mL volume, *n*-hexane (20 mL) was added. The resulting cloudy solution was cooled to 0 °C, and the crystals were filtered, washed with a small amount of cold *n*-hexane and dried under vacuum to give 520 mg (87%) of 2-(benzyloxy)-1-methylpyridinium tetrakis[3,5-bis(trifluoromethyl)phenyl]borate (**1**) as a white solid.

All analytical data were found to be identical to the literature.^[S5,S6]

¹H NMR: δ_{H} (400 MHz, DMSO- d_6) 8.70 (1 H, dd, *J* 6.3, 1.1), 8.56 – 8.49 (1 H, m), 7.83 (1 H, d, *J* 8.8), 7.72 (4 H, br s), 7.62 (8 H, br s), 7.60 – 7.55 (3 H, m), 7.52 – 7.38 (3 H, m), 5.63 (2 H, s), 4.01 ppm (3 H, s);

¹³C NMR: δ_{C} (101 MHz, DMSO- d_6) 161.65, 161.15, 160.66, 160.16, 159.32, 147.67, 143.88, 134.02, 133.74, 129.03, 128.78, 128.23, 125.35, 122.63, 118.56, 117.73, 111.94, 73.37, 41.51 ppm;

¹⁹F NMR: δ_{F} (376 MHz, DMSO- d_6) -61.65 ppm.

Spectral data of the prepared 2-(benzyloxy)-1-methylpyridinium salts

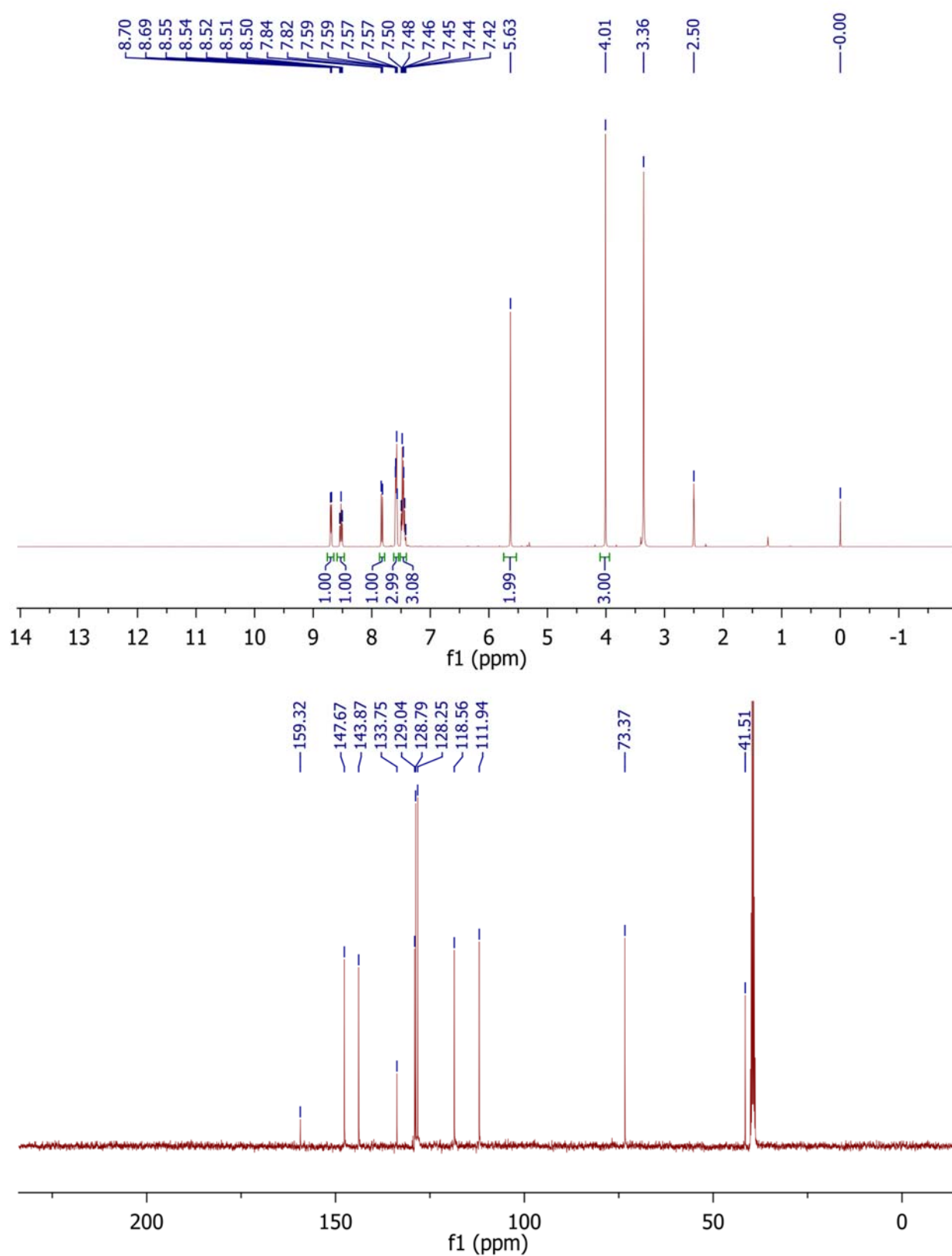


Fig. S12. ¹H-NMR and ¹³C-NMR spectra (400 MHz, DMSO-*d*₆) of 2-(benzyloxy)-1-methylpyridinium trifluoromethanesulfonate (S1).

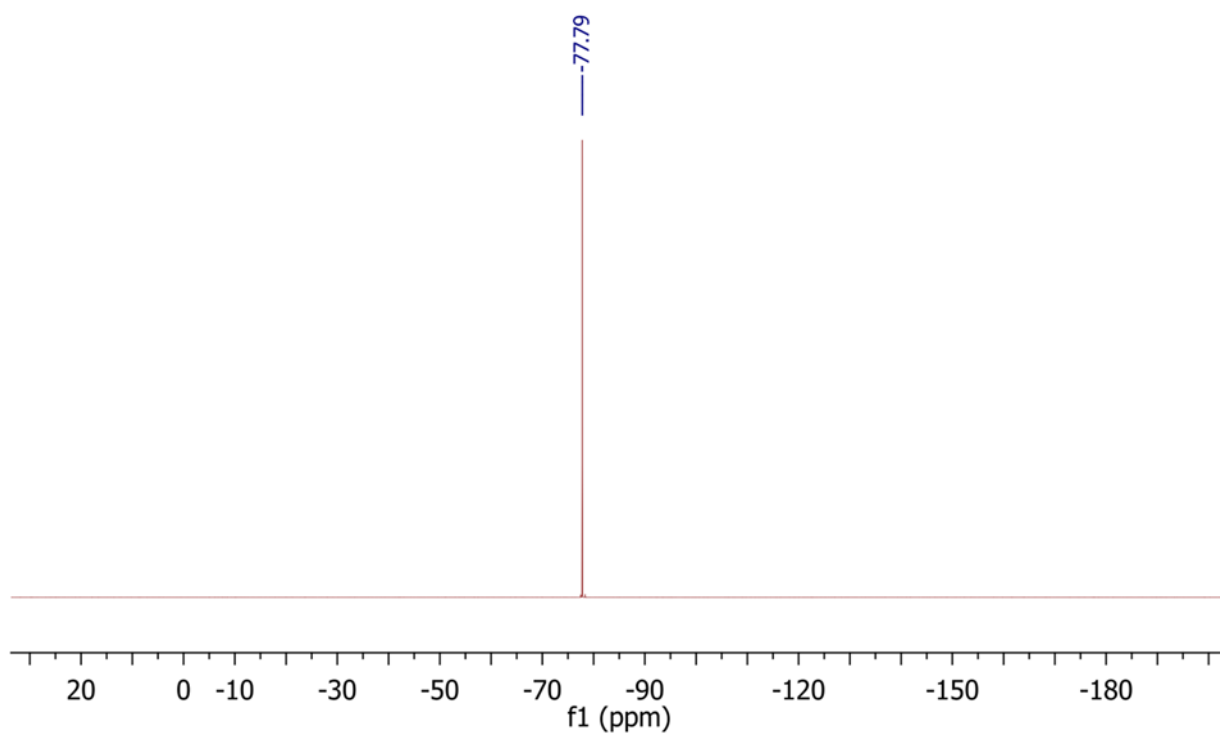


Fig. S13. ^{19}F -NMR spectrum (400 MHz, $\text{DMSO-}d_6$) of 2-(benzyloxy)-1-methylpyridinium trifluoromethanesulfonate (**S1**).

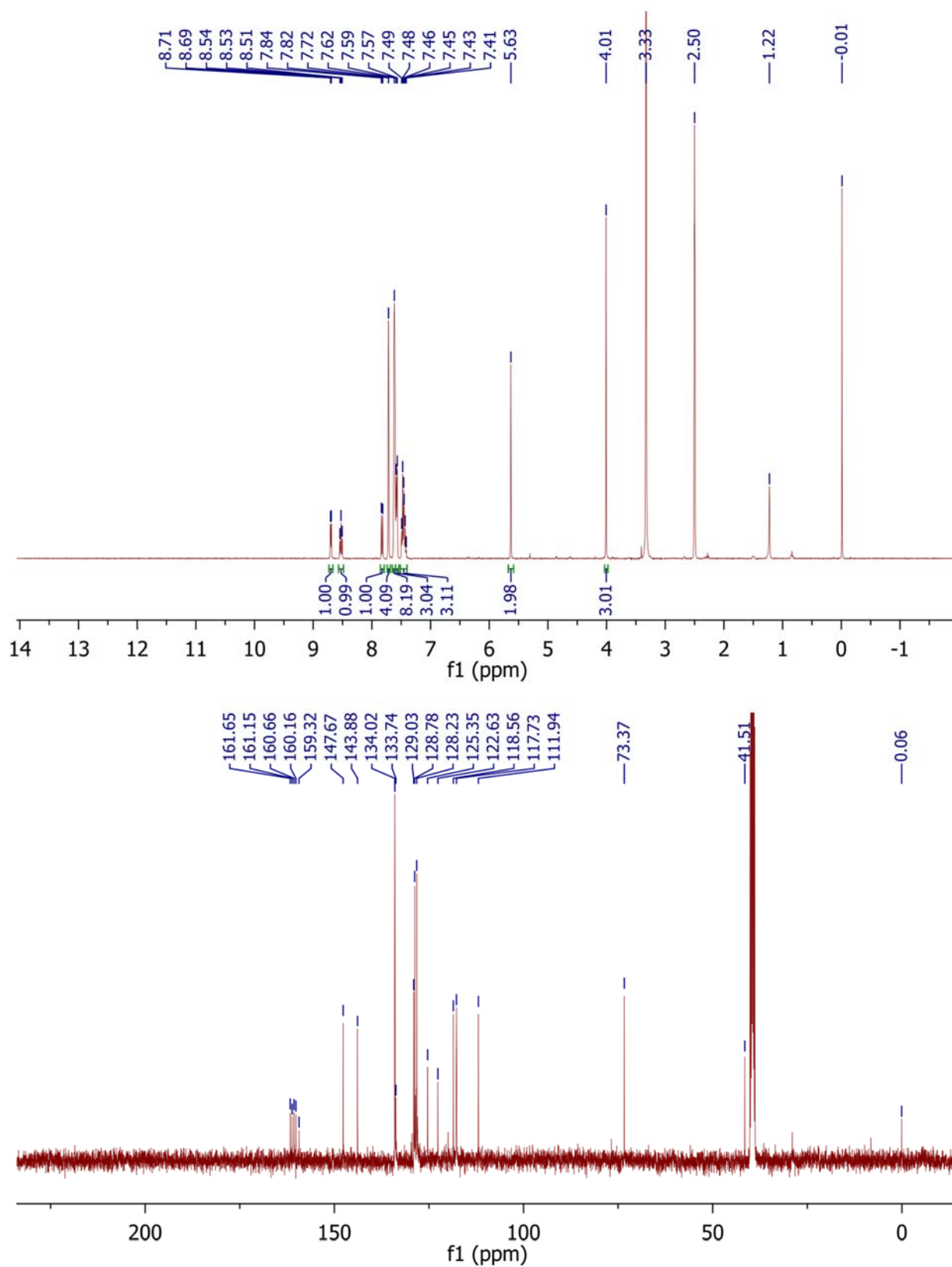


Fig. S14. $^1\text{H-NMR}$ and $^{13}\text{C-NMR}$ spectra (400 MHz, $\text{DMSO-}d_6$) of 2-(benzyloxy)-1-methylpyridinium tetrakis[3,5-bis(trifluoromethyl)phenyl]borate (1).

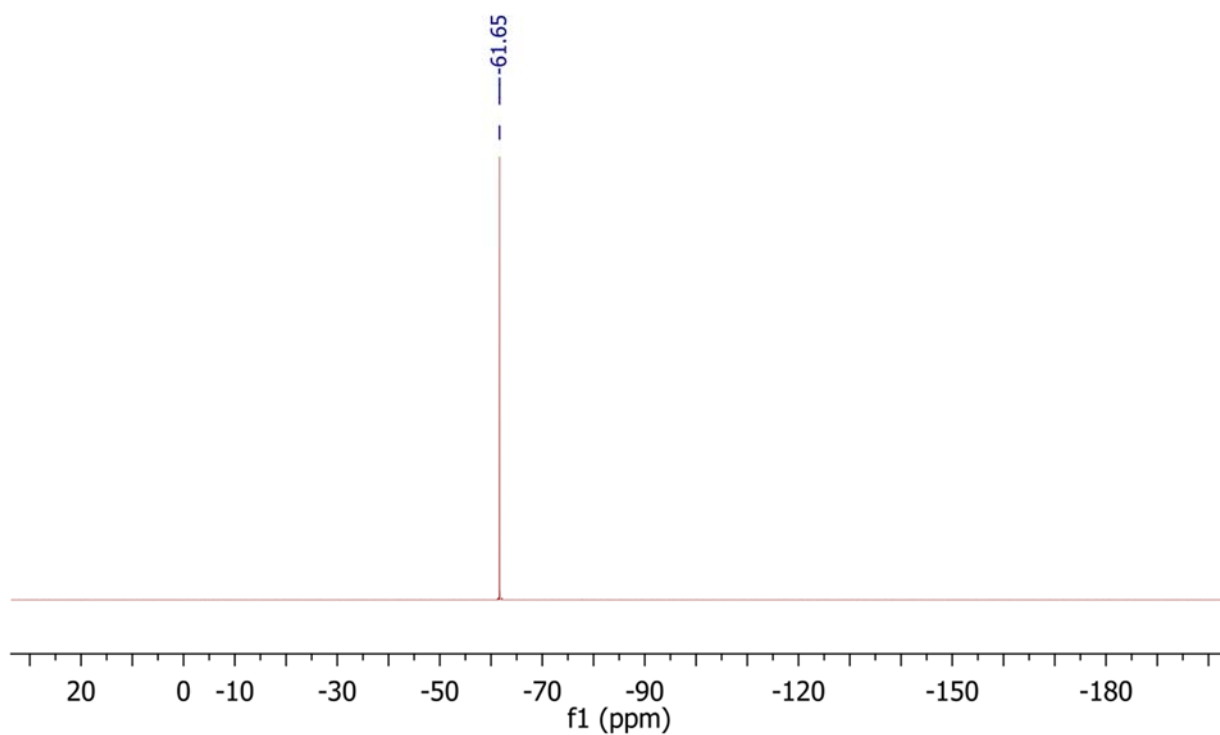


Fig. S15. ^{19}F -NMR spectrum (400 MHz, $\text{DMSO-}d_6$) of 2-(benzyloxy)-1-methylpyridinium tetrakis[3,5-bis(trifluoromethyl)phenyl]borate (1).

MW heating characteristics of the quartz vessels

The MW transparency of the *p*-xylene solvent and quartz ($\tan \delta = 6 \cdot 10^{-5}$) vessels was validated by demonstrating the lack of heating when irradiated with high (300 W) MW power (Fig. S16). Temperature was monitored using internal FO sensor. The low heating rate was comparable to the data published by Kappe using similar conditions.^[S6] Note that the temperature continues to rise after ceasing MW irradiation, which is a consequence of heat transfer from the environment.

For comparison, heating an identical sample inside a Pyrex[®] ($\tan \delta = 10^{-3}$) vessel is also shown (Fig. S16).

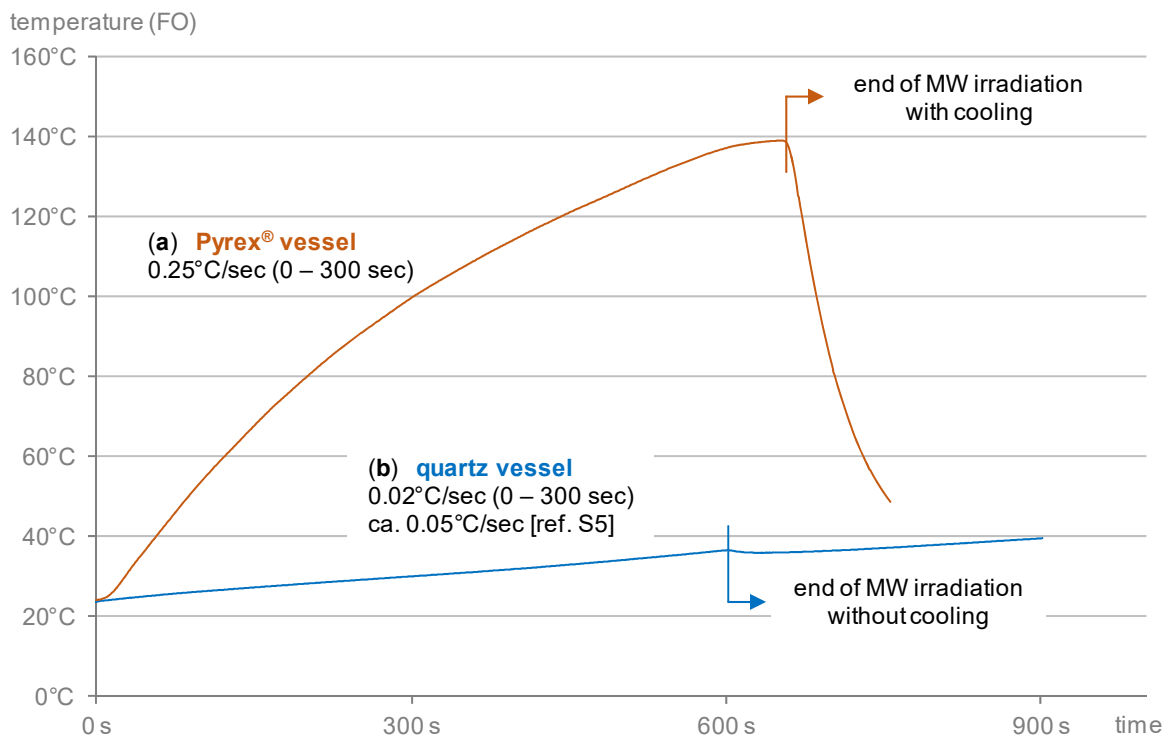
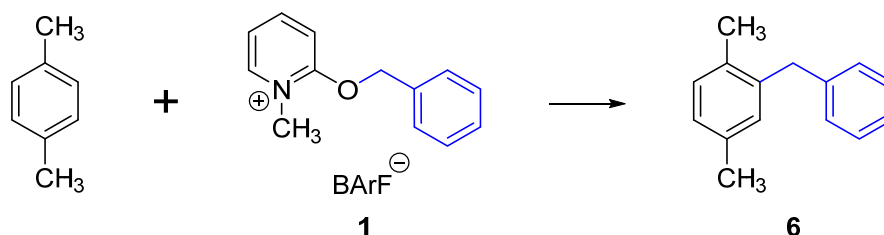


Fig. S16. MW heating profiles (measured by FO sensor) of 10 mL Pyrex[®] (a) and quartz (b) reaction vessels filled with 2.0 mL pure *p*-xylene using 300W constant power without prior conditioning of the MW cavity.

Harmonized temperature profiles in the benzylation of *p*-xylene



Scheme S5. Benzylation of *p*-xylene.

Conventional heating for 30 min total time using pre-heated oil bath (105 °C) was conducted, the obtained inner temperature profile (Fig. S17) was recreated in the MW reactor after extensive experimentation. The set temperature (100 °C) was identical to the steady-state temperature reached in the oil bath experiment, the power settings leading to the best fit are described in Table S2 (entries 1 and 2). The same procedure was repeated with fluoropolymer liner inserted inside the vessels (Fig. S18 and Table S2, entries 3 – 5).

Table S2. Harmonized temperature profiles in the benzylation of *p*-xylene. Average values of parallel experiments (n = 3) are shown in each case except the power setting.

Entry	Heating mode	Vessel	power setting	mean power ^A	heat-up time ^B	mean FO temp. ^A	mean IR temp. ^A
1	Conventional heating (FO monitoring)	Pyrex ^C	–	–	161 s	98.0 °C	–
2	MW heating (FO control)	quartz	60 W	22 W	129 s	98.0 °C	112.3 °C
3	Conventional heating (FO monitoring)	quartz with Teflon [®] PFA liner	–	–	263 s	97.6 °C	–
4	MW heating (FO control)	quartz with Teflon [®] PFA liner	30 W	22 W	280 s	96.2 °C	98.4 °C
5	MW heating (FO control)	quartz with Teflon [®] PFA liner	60 W	27 W	160 s	97.6 °C	99.8 °C

^A Mean value is calculated for the total heating time (0 – 1800 s).

^B Heat-up time is the time interval until reaching 95 °C (measured by FO sensor).

^C Pyrex[®] vessels were used instead of quartz vessels, as the heat transfer and surface characteristics of the two materials are similar, leading to identical results in conventional heating.

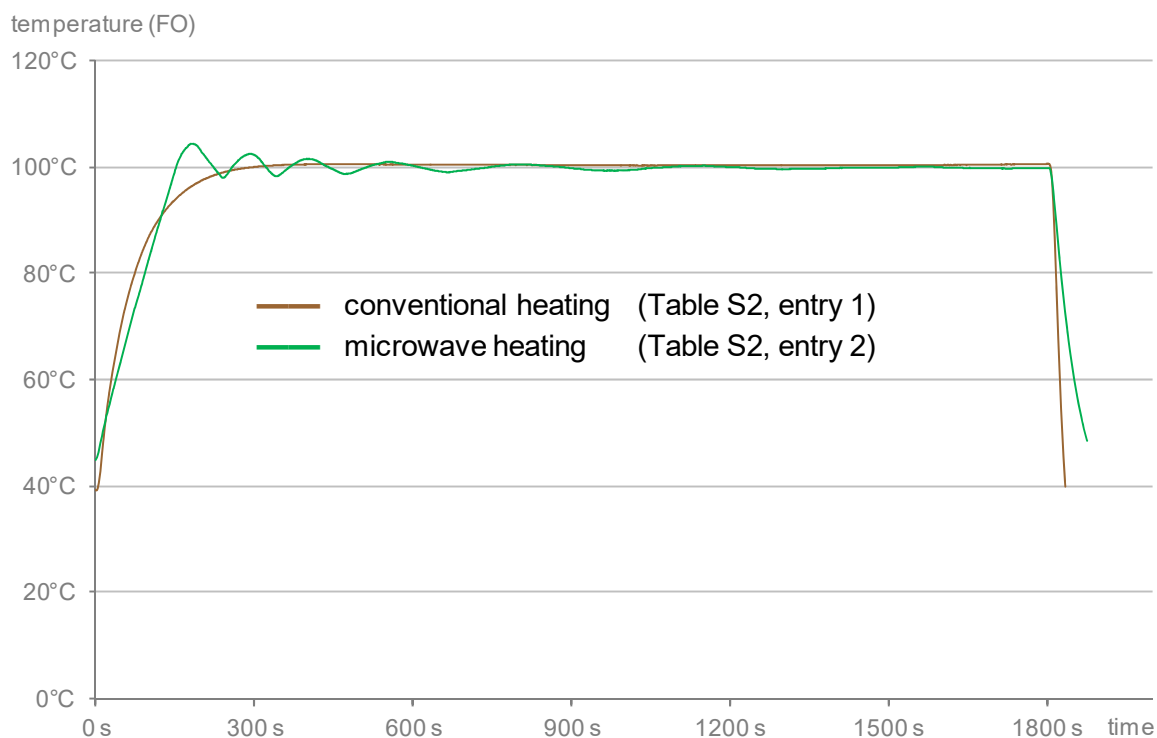


Fig. S17. Comparison of the internal temperature profiles of conventionally and MW heated mixtures of **1** in *p*-xylene. The temperature was measured during the course of the reaction by internal FO sensor. Temperature profiles of the parallel experiments (not shown for clarity reasons) are in good accordance with the displayed profiles.

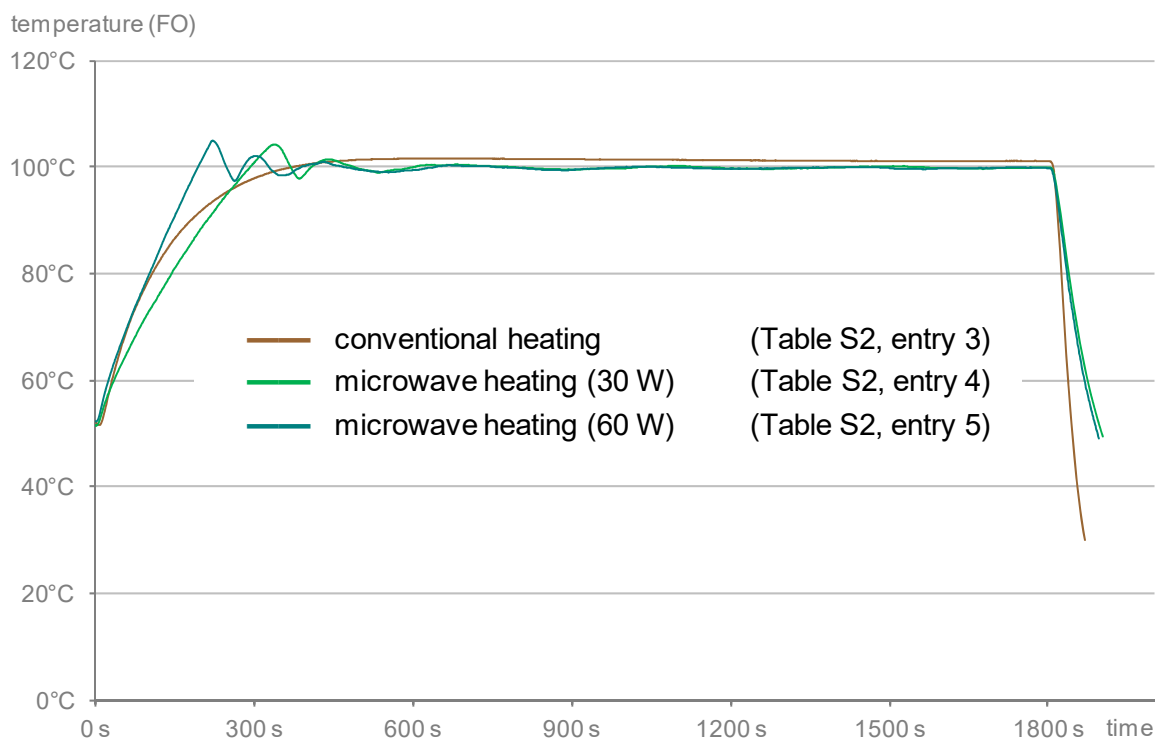


Fig. S18. Comparison of the internal temperature profiles of conventionally and MW heated mixtures of **1** in *p*-xylene using quartz vessels with Teflon® PFA liner. The temperature was measured during the course of the reaction by internal FO sensor. Temperature profiles of the parallel experiments (not shown for clarity reasons) are in good accordance with the displayed profiles.

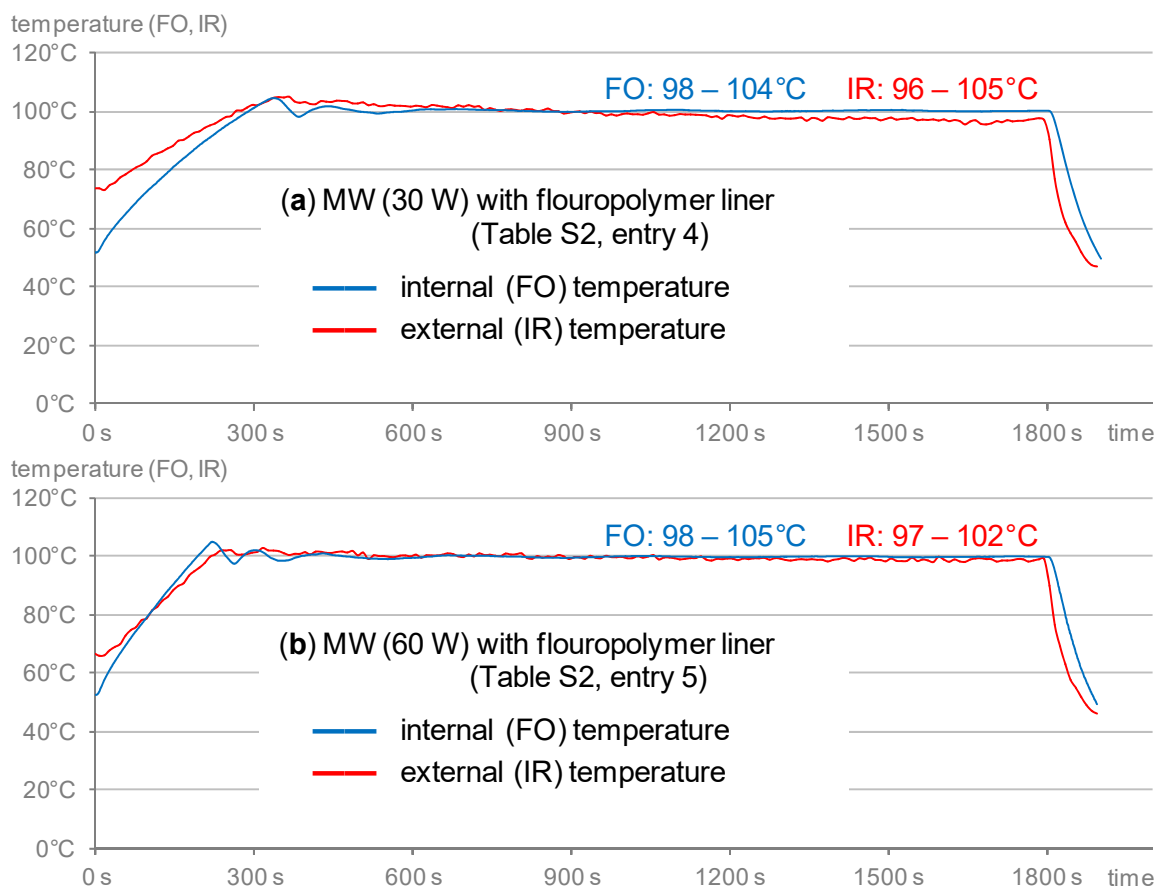


Fig. S19. Comparison of the **internal (FO)** and **external (IR)** temperature profiles of MW heated mixtures of **1** in *p*-xylene using 30 W **(a)** and 60 W **(b)** initial power in quartz vessels with Teflon® PFA liners. The IR values are averaged over 10 sec intervals to decrease measurement noise. Both FO and IR temperature profiles of the parallel experiments (not shown for clarity reasons) are in good accordance with the displayed profiles.

The range of FO and IR temperature values after reaching target temperature are shown on the plots.

Analysis of the reaction mixtures of the benzylation of *p*-xylene

Decomposition of the reagent (associated with water content^[S6] in DMSO-*d*₆ solutions) was not observed in any of the samples prepared with use of CDCl₃.

Conversion based on the ¹H-NMR spectra of the crude (*p*-xylene solution) reaction mixtures (Fig. S20) was calculated using the integrated intensity (*I*) of peaks corresponding to benzyl protons at 3.82 ppm (product, **6**, C-CH₂-Ph) and 4.69 ppm (reagent, **1**, O-CH₂-Ph):

$$\text{conversion(\%)} = \frac{I(\mathbf{6}, \text{C} - \text{CH}_2 - \text{Ph})}{I(\mathbf{6}, \text{C} - \text{CH}_2 - \text{Ph}) + I(\mathbf{1}, \text{O} - \text{CH}_2 - \text{Ph})}$$

Alternatively, conversion could also be calculated from the crude (*p*-xylene solution) reaction mixtures using the *N*-methyl signals at 2.98 ppm (reagent, **1**, N-CH₃), 3.14 ppm (*N*-methyl-2-pyridone, **7**, N-CH₃), 3.36 ppm (*N*-methyl-2-hydroxypyridinium salt, **8**, N-CH₃):

$$\text{conversion(\%)} = \frac{I(\mathbf{7}, \text{N} - \text{CH}_3) + I(\mathbf{8}, \text{N} - \text{CH}_3)}{I(\mathbf{7}, \text{N} - \text{CH}_3) + I(\mathbf{8}, \text{N} - \text{CH}_3) + I(\mathbf{1}, \text{N} - \text{CH}_3)}$$

Representative spectra of the precise comparison experiments are shown on Fig. S21 – S22.

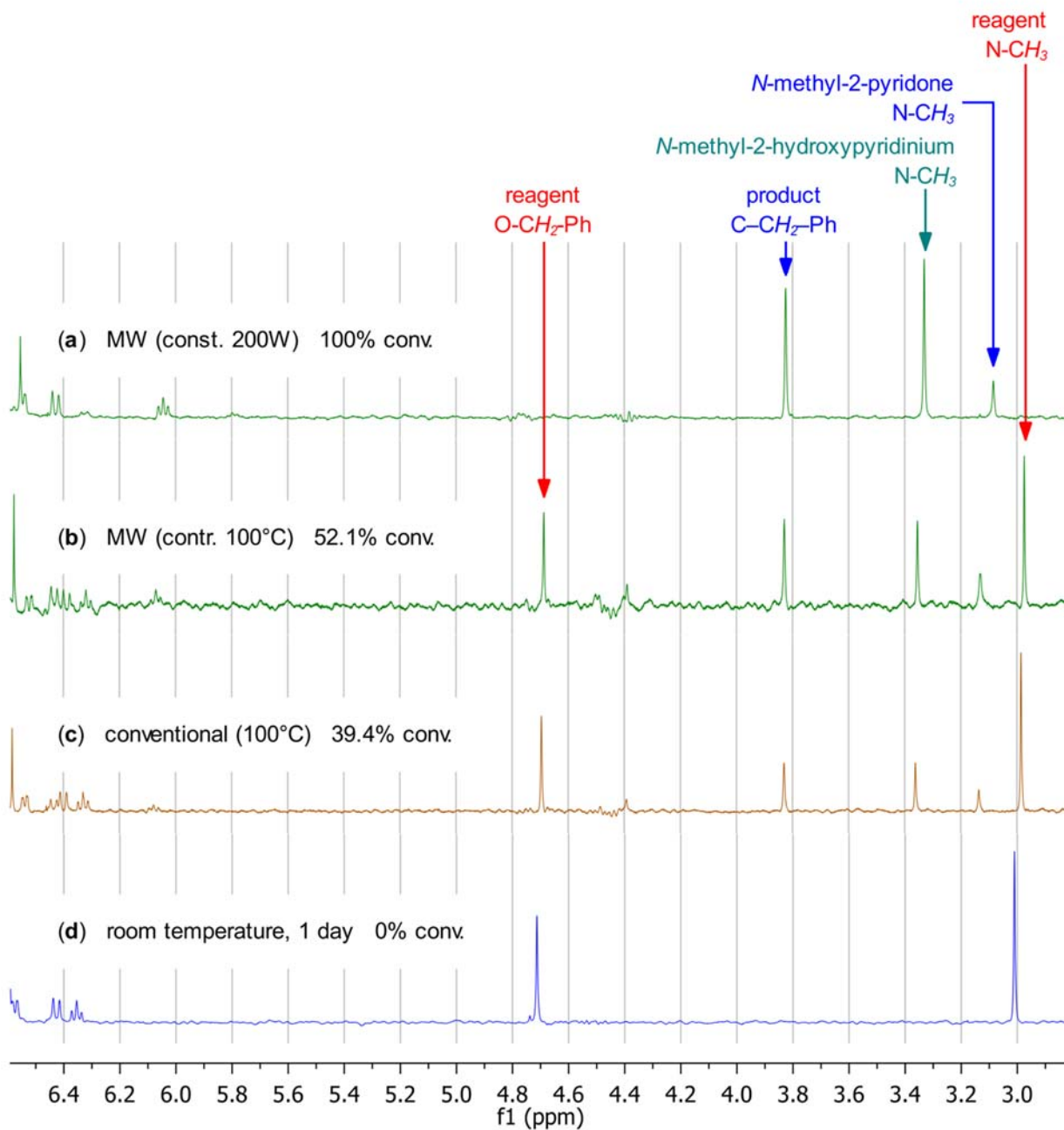


Fig. S20. 1H -NMR spectra (6.6 – 2.8 ppm, not including the signal of the *p*-xylene solvent) of crude reaction mixtures of the MW (200 W constant power) heated for 30 min (a), FO controlled MW (200 W) heated at 100 °C for 30 min (b), conventionally heated at 100 °C for 30 min (c) experiments of the benzylation of *p*-xylene and the reaction mixture kept at room temperature for 1 day (d). The diagnostic signals are marked.

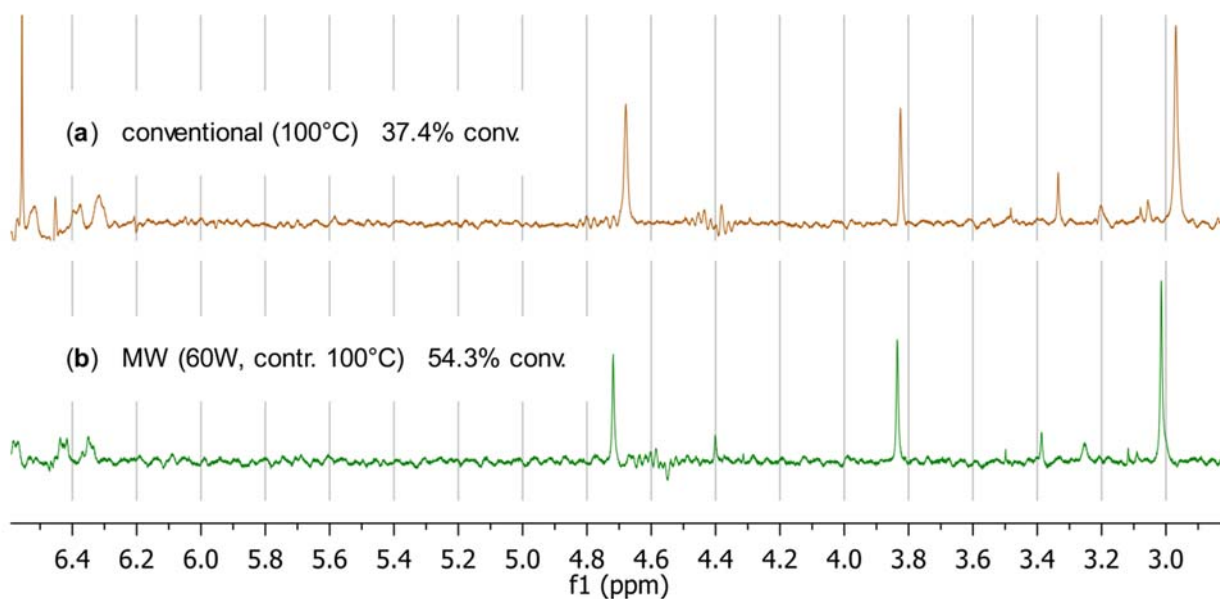


Fig. S21. Representative ^1H -NMR spectra (6.6 – 2.8 ppm) of crude reaction mixtures of the conventionally heated (a) and FO controlled MW (60 W) heated (b) experiments of the benzylation of *p*-xylene (conditions: 100 °C set temperature, 30 min total time).

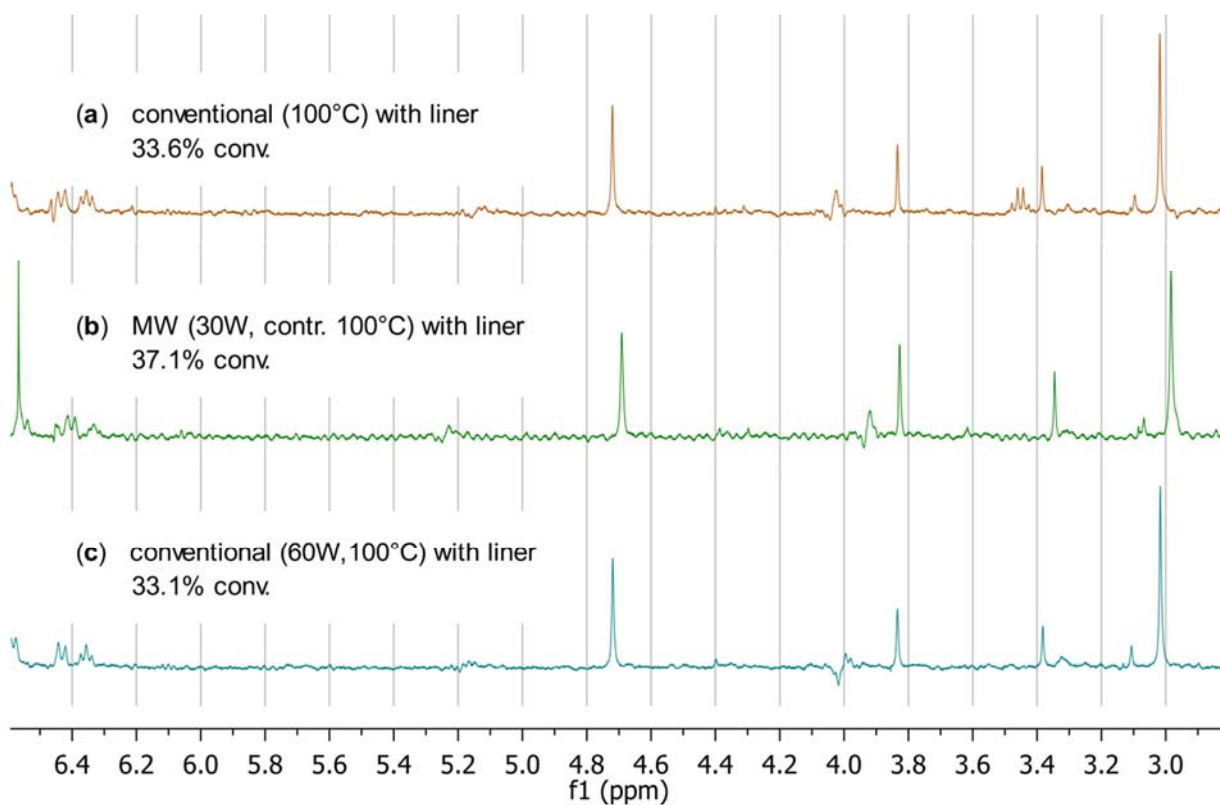


Fig. S22. Representative ^1H -NMR spectra (6.6 – 2.8 ppm) of crude reaction mixtures of the conventionally heated (a), FO controlled MW (30 W) heated (b) and FO controlled MW (60 W) heated (c) experiments of benzylation of the *p*-xylene using fluoropolymer liner (conditions: 100 °C set temperature, 30 min total time).

Observation of 1,3-bis(trifluoromethyl)benzene (9) in the vapors

The presence of the hypothesized volatile (boiling point^[S7]: 116 °C) 1,3-bis(trifluoromethyl)benzene (**9**) by-product could be verified by analysis of the vapors exiting the reaction mixtures, in cases with temperatures close to boiling point of the solvent.

BnOP-BArF (**1**; 10.0 mg, 0.0094 mmol) was added into a dry Pyrex[®] MW vessel equipped with a stir bar, then *p*-xylene (anhydrous, ≥99%; 2.0 mL) was added. A heat gun was used to gently heat the tube while stirring until the solids were completely dissolved. A FO probe was inserted and the vessel was sealed by the locking cover assembly, which was open to the atmosphere through a small vial to trap the vapors exiting the apparatus.

The reaction mixture was heated by constant 200 W MW power while stirring ('High' setting, ca. 700 rpm) for 30 min total time. Internal temperature (monitored by FO probe) reached 139 °C (within 2 min), after 10 min the emerging vapors condensed in the trap at a steady rate.

After the prescribed reaction time, the mixture was cooled down. Conversion determined from the crude reaction mixture was 100%.

The distillate (0.1 mL) was diluted with CDCl₃ (0.7 mL) and subjected to ¹H-NMR analysis, which revealed small amount (0.13%) of 1,3-bis(trifluoromethyl)benzene (**9**) besides the *p*-xylene solvent. Independently, the distillate (50 μL) diluted with methanol (0.5 mL) was analyzed by GC-FID, which showed comparable amount (0.17%) of **9** and *p*-xylene. Identification was verified by comparison to authentic samples of **9** mixed with *p*-xylene in similar ratio for both methods.

Spectral data of the product (6) of the benzylation of p-xylene

The ¹H-NMR spectrum (Figure S23) of a purified sample of the reaction product (**6**) was identical to that of literature reports.^[S8]

¹H NMR: δ_H (400 MHz, CDCl₃) 7.30 – 7.23 (2 H, m), 7.21 – 7.14 (1 H, m), 7.12 (2 H, d, *J* 7.1), 7.05 (1 H, d, *J* 7.6), 6.98 – 6.90 (2 H, m), 3.95 (2 H, s), 2.28 (3 H, s), 2.19 ppm (3 H, s).

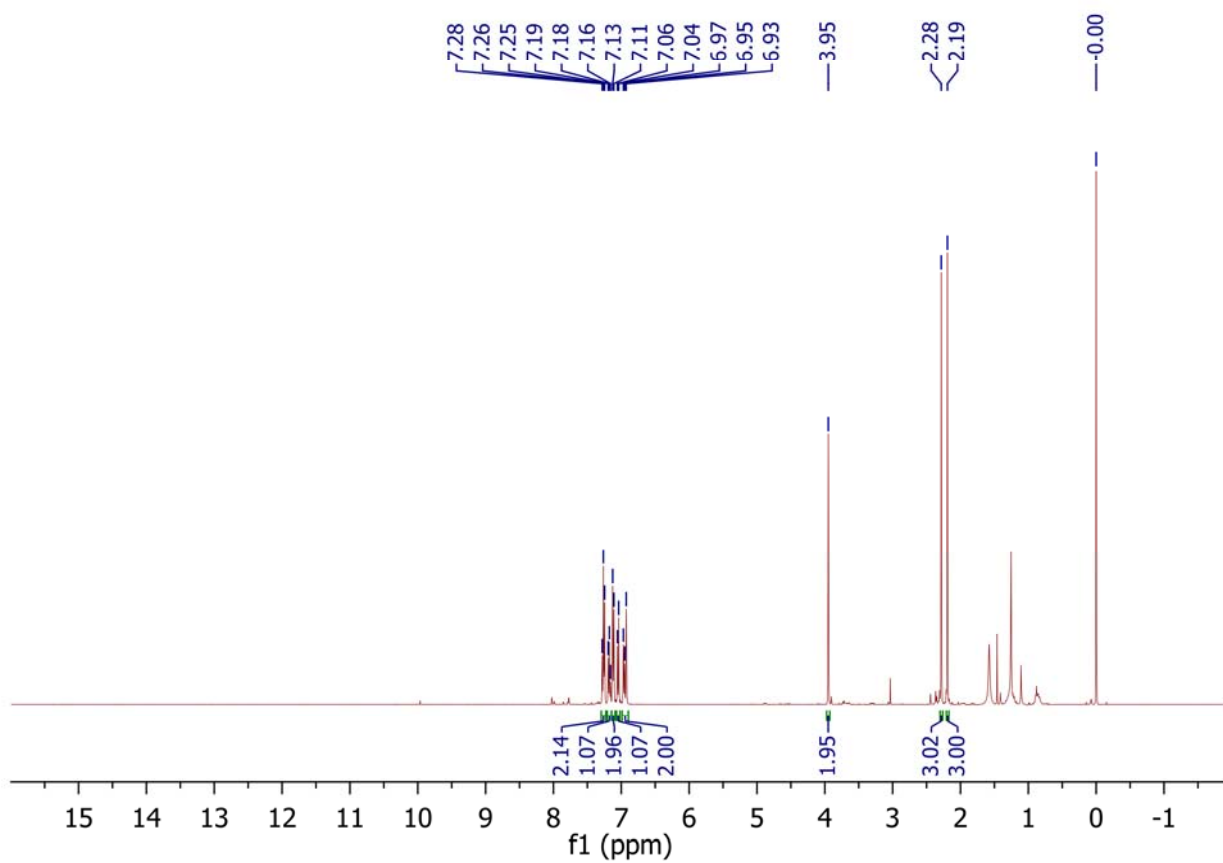


Fig. S23. $^1\text{H-NMR}$ spectrum (400 MHz, CDCl_3) of a purified sample of the product (**6**) of the benzylation of *p*-xylene. Residual solvents (signals in the range of 2 – 0.5 ppm) could not be fully removed after chromatography, because of the volatility of the product.

References

- [S1] K. Poon, P. Albinia, G. Dudley, *Org. Synth.* **2007**, *84*, 295. doi:10.15227/orgsyn.084.0295
- [S2] P. Bana, I. Greiner, *Aust. J. Chem.* **2016**, *69*, 865. doi:10.1071/ch16017
- [S3] E. L. Lanni, M. A. Bosscher, B. D. Ooms, C. A. Shandro, B. A. Ellsworth, C. E. Anderson, *J. Org. Chem.* **2008**, *73*, 6425. doi:10.1021/jo800866w
- [S4] K. W. C. Poon, G. B. Dudley, *J. Org. Chem.* **2006**, *71*, 3923. doi:10.1021/jo0602773
- [S5] M. R. Rosana, Y. Tao, A. E. Stiegman, G. B. Dudley, *Chem. Sci.* **2012**, *3*, 1240. doi:10.1039/c2sc01003h
- [S6] C. O. Kappe, B. Pieber, D. Dallinger, *Angew. Chem. Int. Ed.* **2013**, *52*, 1088. doi:10.1002/anie.201204103
- [S7] H. Freiser, M. E. Hobbs, P. M. Gross, *J. Am. Chem. Soc.* **1949**, *71*, 111. doi:10.1021/ja01169a030
- [S8] C. L. Ricardo, X. Mo, J. A. McCubbin, D. G. Hall, *Chem. Eur. J.* **2015**, *21*, 4218. doi:10.1002/chem.201500020